

Melamine Driven Supramolecular Self-Assembly of Nucleobase Derivatives in Water

Yan Xiao , Jiaxiao Zhang, Meidong Lang

Shanghai Key Laboratory of Advanced Polymeric Materials, Key Laboratory for Ultrafine Materials of Ministry of Education, School of Materials Science and Engineering, East China University of Science and Technology, Shanghai 200237, China
Correspondence to: Y. Xiao (E-mail: yxiao@ecust.edu.cn) or M. Lang (E-mail: mdlang@ecust.edu.cn)

Received 3 November 2017; accepted 2 January 2018; published online 00 Month 2018

DOI: 10.1002/pola.28954

ABSTRACT: Water-soluble supramolecular polymers, especially made up of biomolecules, are ideally suited to build new biomaterials that can mimic or interact with dynamic, biological environments. Here, two derivatives from thymine (T), that is *N*-[2-(3,4-Dihydro-5-methyl-2,4-dioxo-1(2H)-pyrimidinyl)acetyl]-L-phenylalanine (T-phe) and *N*-(2-Aminoethyl)-3,4-dihydro-5-methyl-2,4-dioxo-1(2H)-pyrimidineacetamide (T-NH₂) were synthesized. Then the optimal condition for self-assembly of T-phe and T-NH₂ driven by melamine (M) was explored. It was observed that M/T kept at 1:3 with equivalent T-phe and T-NH₂ under neutral environment resulted in long fibers (>1 μm) with extremely high aspect ratios, which suggested that electrostatic and π-stacking interactions could be effectively orchestrated by

hydrogen bonds to direct the hierarchical assembly. Furthermore, hydrogels were spontaneously generated with a concentrated solution of T-phe, T-NH₂, and M due to the fibril entanglement. Given its biomimetic nature and efficient self-assembly process, this newly developed supramolecular polymer stacked by tetrameric structures represented an innovative concept and pathway for novel bio-inspired materials. © 2018 Wiley Periodicals, Inc. *J. Polym. Sci., Part A: Polym. Chem.* 2018, 00, 000–000

KEYWORDS: fiber; melamine; nucleobase derivatives; supramolecular polymer; water-soluble

INTRODUCTION Rapid progress has been made in supramolecular polymers since Lehn and coworkers firstly reported that bifunctional diamidopyridines and uracil derivatives formed linear chains via intermolecular force.¹ Different from conventional polymers linked by covalent bonds of repeating units, supramolecular polymers are held together by highly directional and reversible non-covalent interactions, including coordination, hydrogen bond, π-π interaction, and so on.^{2–4} Among them, hydrogen bonding is considered as one of the most versatile interactions in fabrication of functional materials due to its specificity and directionality. For instance, poly(ethylene/butylene) functionalized with self-complementary quadruple hydrogen-bonded ureido-pyrimidone (UPy) units preserved the combinational advantages of excellent mechanical properties and feasible processibility.⁵ However, H-bonding usually weakens under polar conditions like in water, where assemblies purely based on H-bonds become unstable.⁶ Therefore, a hydrophobic microenvironment is usually built for H-bonding motifs to promote their assembling in water.⁷ For example, hydrophilic polyethylene glycol (PEG) end-capped with UPy units could not self-assemble into the nanofibers unless a

hydrophobic alkyl pocket was spaced and shielded.⁸ Boué and coworkers reported that alkylene spacers were placed in between bis-urea motif and water-soluble ethylene oxide oligomers to create a hydrophobic environment and thereby formed long rigid filaments.⁹ Alternatively, electrostatic or π-stacking interactions were more often combined with hydrogen bonding to obtain stable assemblies, owing to the strong non-covalent force.^{10–12} Besenius and coworkers mixed the oppositely charged dendritic peptide amphiphiles in a 1:1 ratio to supramolecular copolymers through a combination of Coulomb attractive forces and hydrogen-bonding interactions.¹³ Lloyd and coworkers reported that a family of aromatic carboxylic acid benzene 1,3,5-tricarboxamide (BTA) modifications showed spontaneous nucleation and one-dimensional growth resulting from the molecules stacking into fibers through π-stacking interactions and amide–amide hydrogen bonding.¹⁴

In nature, molecular recognition including duplex DNA *via* Watson–Crick base-pairing is ubiquitous. Such specific interaction is originated from non-covalent bonding between two or more biomolecules. Over the last few decades, chemists have been to go beyond the natural realm and to use

Additional Supporting Information may be found in the online version of this article.

© 2018 Wiley Periodicals, Inc.

complementary nucleobase-pairing to construct novel supramolecular assemblies.¹⁵ Fenniri and colleagues pioneered the supramolecular polymers with the heteroaromatic bicyclic base G \wedge C, which resulted in remarkable helical rosette nanotubes.^{16–18} Zhu et al. reported that adenine-terminated poly(ϵ -caprolactone) and uracil-terminated poly(ethylene glycol) assembled in water on association of their complementary termini to form well-defined micelles capable of doxorubicin uptake.¹⁹ However, small molecules including canonical nucleobases and their corresponding mononucleosides do not form H-bonded base-pairing in water.²⁰ A notable exception is the G-tetrad formed by guanosine compounds with the aid of cation coordination, leading to polymeric structures in water and ultimately hydrogels.^{21,22} Such stable assemblies were attributed to the hydrophobic surface with an area greater than about 1 nm², which was beneficial for stacking to build supramolecular polymers.²³ Therefore, the combination of nucleobases with other moieties was necessary to enlarge the hydrophobic surface and thereby access higher-order supramolecular structure in water.²⁴ Recently, Sleiman and coworkers have reported that cyanuric acid (CA) with three thymine-like faces reprogrammed the assembly of unmodified poly(adenine) (poly(A)) into long and abundant fibers with cyclic hexamers as internal structure.²⁵ Hud et al. have demonstrated that adenosine-5'-monophosphate (AMP) was able to form supramolecular assemblies of stacked hexads with CA in water.²⁶ Up to date, most existing supramolecular polymers based on nucleobases have focused on six-membered supermacrocycles as intermediate structure.

Melamine (M) is a versatile molecule as scaffolding components in the field of supramolecular chemistry due to its nine H-bonding sites and aromatic planar ring structure.²⁷ Zhang et al. reported the synthesis of 2D organic micro sheets using dialkylated M derivatives with halogen acid.²⁸ Kitamura et al. developed a well-defined columnar structure based on CA-functionalized perylene bisimide and substituted M.²⁹ Among the natural nucleobases, thymine (T) contains complementary NH \cdots O and NH \cdots N hydrogen bonds with M.³⁰ Intrigued by this recognition unit, Liu et al. synthesized amphiphilic polystyrene-co-poly(*N*-acryloylthymine), which could be used for detecting M.³¹ Besides, Bong et al. reported that M-displaying α -peptides were able to mediate discrete assembly of T-rich DNA/RNA.^{32–34} However, this molecular recognition has rarely been applied to supramolecular polymer in aqueous environment owing to poor water-solubility of T and M.

In this paper, two derivatives from T, bearing terminal amide and carboxyl groups respectively, were proposed. M was expected to drive self-assembly of nucleobase derivatives in water to build supramolecular assembly by the combinational interactions of H-bonds, π -stacking, and Coulomb attractive forces. The optimal condition of self-assembly in water was extensively investigated. The fibrillar structures were observed and mechanism of self-assembly was further suggested. We also expected to fabricate hydrogel based on the self-assembled system in concentrated solution.

EXPERIMENTAL

Materials

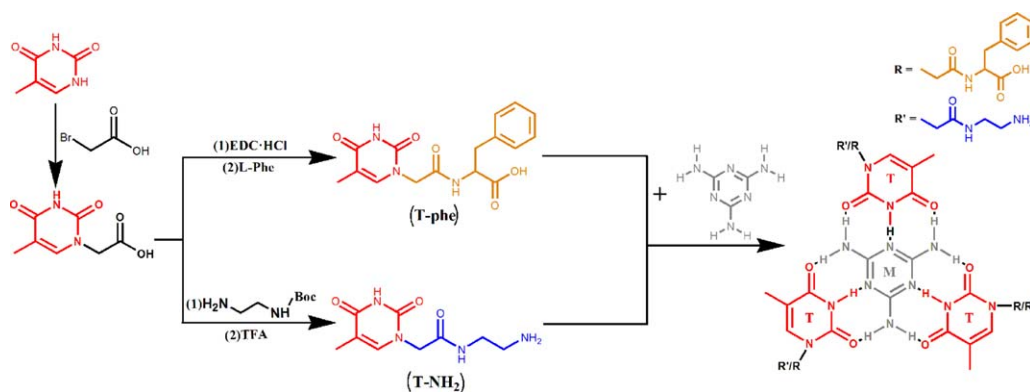
Thymine (99%), bromoacetic acid (99%), L-phenylalanine (98%), and *N*-Boc-ethylenediamine (98%) were purchased from Aladdin reagent and used without further purification. *N,N*-Dimethylformamide (DMF) was refluxed with calcium hydride (CaH₂) and distilled in vacuum. 1-Ethyl-3-(3-dimethyl-aminopropyl)-1-carbodiimide hydrochloride (EDC·HCl) and *N*-hydroxysuccinimide (NHS) were purchased from Aldrich and used as received. All other reagents and solvents were purchased from Aladdin and used without further purification.

General Characterization

¹H NMR (400 MHz) spectra in dimethyl sulfoxide (DMSO-*d*₆) and ¹³C NMR (100 MHz) spectra in deuterioxide (D₂O) were recorded at room temperature on a Bruker Avance series instrument. UV/Vis absorbance spectra were recorded on a Perkin Elmer Lambda Bio40 UV spectrometer with different concentration. Dynamic light scattering (DLS) measurements were carried out using a Brookhaven BI-200SM goniometer equipped with a BI-9000AT digital correlator. The aggregates in aqueous solution were filtered through a 0.45 μ m cellulose membrane filter before analysis. Potentiometric Titrant (ZDJ-4A) was used to measure the p*K*_a values of both T-phe and T-NH₂. 0.01 mol·L⁻¹ NaOH and HCl were used as standard titrated solution of T-phe and T-NH₂, respectively. The end point of titration was determined by the jump of pH value. AFM imaging was performed on freshly cleaved mica using a MultiMode 8 microscope with a Nanoscope V controller (Bruker) in ScanAsyst mode. A 5- μ l mixture solution was dropped and dried at 15 °C overnight. TEM (JEOL/JEM-1400EXII) was used to observe the morphology of the aggregates at an acceleration voltage of 60 keV. Typically, a drop of mixture solution was added on the copper grid followed by drying at room temperature before observation. The ESI mass spectra were recorded in CH₃OH/H₂O (1/1) with a Bruker Daltonics microTOFTM focus spectrometer. SEM (S-4800N) was used to investigate the morphology of the hydrogels. The hydrogel samples were put on the silicon wafer and dried at room temperature overnight.

Synthesis of (Thymine-1-yl) Acetic Acid

According to the literature, a typical procedure for synthesis of (thymine-1-yl) acetic acid was described as follows.³⁵ Thymine (3.78 g, 30 mmol) was dissolved in 20 ml KOH (6.458 g, 115 mmol) aqueous solution, which was then kept at 40 °C. Afterwards, a solution of bromoacetic acid (6.25 g, 45 mmol) in deionized water (10 ml) was slowly added over 30 min. The reaction mixture was stirred for another 30 min at 40 °C. Then it was cooled to room temperature and pH was adjusted to 5.5 with HCl. The solution was then put in a refrigerator for 2 h. Any precipitate formed was removed by filtration. The solution was then adjusted to pH 2 with HCl and put in a freezer for 2 h. The resultant white precipitate was isolated by filtration, washed with water and dried to afford the white product. ¹H NMR (400 MHz, DMSO-*d*₆, δ): 7.50 (s, —C(CH₃)=CH—), 4.37 (s, —CH₂COOH), 1.76 (s, —C(CH₃)=CH—). ¹³C NMR (100 MHz, D₂O, δ): 11.9



SCHEME 1 Syntheses of T-NH₂ (+), T-phe (-) and hydrogen-bonding recognition between melamine (M) and thymine (T). [Color figure can be viewed at wileyonlinelibrary.com]

($-\text{C}(\text{CH}_3)=\text{CH}-$), 51.4 ($-\text{CH}_2\text{COOH}$), 111.3 ($-\text{C}(\text{CH}_3)=\text{CH}-$), 141.8 ($-\text{C}(\text{CH}_3)=\text{CH}-$), 160.0 ($-\text{CH}_2\text{COOH}$), 176.4, 177.6 ($-\text{CONHCO}-$).

Synthesis of *N*-[2-(3,4-Dihydro-5-Methyl-2,4-Dioxo-1(2H)-Pyrimidinyl)Acetyl]-L-Phenylalanine (T-phe)

According to the literature, (thymine-1-yl) acetic acid (184 mg, 1 mmol) was added to a 25 ml Schlenk flask followed by addition of 10 ml dry DMF.³⁶ After the solid was completely dissolved in DMF, EDC-HCl (210.9 mg, 1.1 mmol) and NHS (126.5 mg, 1.1 mmol) were introduced and stirred at room temperature for 1 h. L-Phenylalanine (166 mg, 1 mmol) and Na₂CO₃ (84.8 mg, 0.8 mmol) were dissolved in 20 ml of water with stirring and added to the above DMF solution. The resulted reaction mixture was stirred at room temperature for 24 h followed by vacuum drying. Then 30 ml of deionized water was added and acidified to pH 3, the resulted product was obtained by filtration, washed with deionized water, and then dried *in vacuo*. The white solid was purified by HPLC using water-acetonitrile as eluent (from 8:2 to 4:6). ¹H NMR (400 MHz, DMSO-*d*₆, δ): 8.55 (s, $-\text{CH}_2\text{CONH}-$), 7.45 (m, $-\text{C}(\text{CH}_3)=\text{CH}-$), 7.35 (m, Ph-*H*), 4.43 (m, $-\text{NHCH}(\text{COOH})\text{CH}_2-$), 4.19 (m, $-\text{CH}_2\text{CONH}-$), 3.04, 2.89 (dd, $-\text{CH}_2\text{Ph}$), 1.73 (s, $-\text{C}(\text{CH}_3)=\text{CH}-$). ¹³C NMR (100 MHz, D₂O, δ): 11.8 ($-\text{C}(\text{CH}_3)=\text{CH}-$), 37.6 ($-\text{CH}_2\text{Ph}$), 55.9 ($-\text{CH}_2\text{CONH}-$), 59.3 ($-\text{NHCH}(\text{COOH})\text{CH}_2-$), 111.3 ($-\text{C}(\text{CH}_3)=\text{CH}-$), 126.8, 128.6, 129.0, 135.2 (Ar), 142.2 ($-\text{C}(\text{CH}_3)=\text{CH}-$), 160.0 ($\text{NHCH}(\text{COOH})\text{CH}_2-$), 169.4 ($-\text{CH}_2\text{CONH}-$), 177.2, 177.8 ($-\text{CONHCO}-$).

Synthesis of *N*-(2-Aminoethyl)-3,4-Dihydro-5-Methyl-2,4-Dioxo-1(2H)-Pyrimidineacetamide (T-NH₂)

(Thymine-1-yl) acetic acid (184 mg, 1 mmol) was added into a 25 ml Schlenk flask followed by addition of 10 ml dry DMF. After the solid was dissolved in DMF completely, EDC-HCl (210.9 mg, 1.1 mmol) and NHS (126.5 mg, 1.1 mmol) were introduced and stirred at room temperature for 1 h. *N*-Boc-ethylenediamine (160 mg, 1 mmol) was added to the above DMF solution. The resulted reaction mixture was stirred at room temperature for 24 h and then vacuum-dried. 2 ml DCM and 1 ml TFA were added into the reaction mixture, which was kept stirring at room temperature for

1 h and vacuum dried. Then 30 ml of deionized water was added and basified to pH 11, the resulted solution was obtained by filtration. After evaporation, the product was

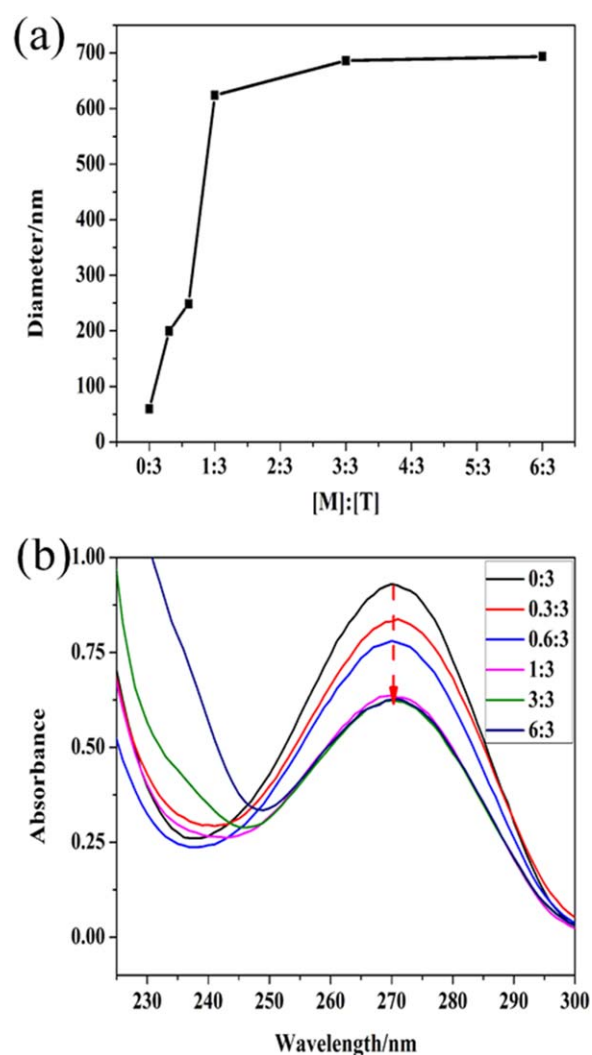


FIGURE 1 (a) Diameters from DLS and (b) UV spectra of mixture of M/T at different molar ratios: 0:3, 0.3:3, 0.6:3, 1:3, 3:3, and 6:3. [Color figure can be viewed at wileyonlinelibrary.com]

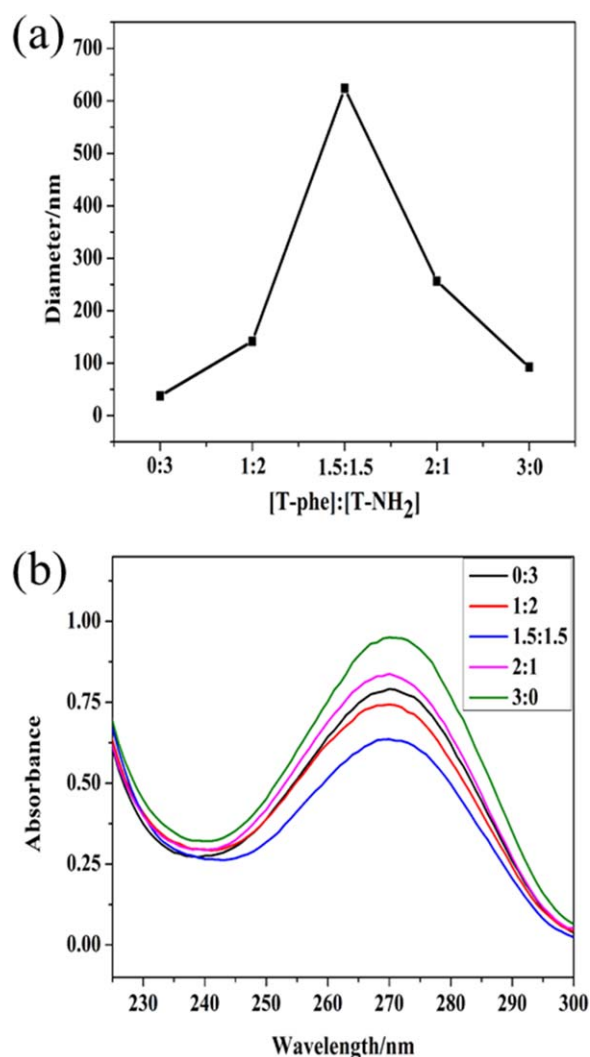


FIGURE 2 (a) Diameters from DLS, (b) UV spectra of mixture of T-phe and T-NH₂ with M while the molar ratio of T-phe and T-NH₂ was different in phosphate buffer. [Color figure can be viewed at [wileyonlinelibrary.com](#)]

recrystallized from methanol as purified and colorless material. ¹H NMR (400 MHz, DMSO-*d*₆, δ): 8.53 (s, -CH₂CONH-), 7.50 (d, -C(CH₃)=CH-), 4.34 (s, -CH₂CONH-), 3.35 (-CH₂CH₂NH₂ + H₂O), 2.86 (t, -CH₂CH₂NH₂), 1.75 (s, -C(CH₃)=CH-). ¹³C NMR (100 MHz, D₂O, δ): 11.2 (-C(CH₃)=CH-), 36.9 (-CH₂CH₂NH₂), 39.0 (-CH₂CH₂NH₂), 50.6 (-CH₂CONH-), 111.0 (-C(CH₃)=CH-), 143.1 (-C(CH₃)=CH-), 152.3, 166.9 (-CONHCO-), 170.2 (-CH₂CONH-).

RESULTS AND DISCUSSION

Synthesis and Characterization

Two derivatives of thymine (T), *i.e.* *N*-[2-(3,4-Dihydro-5-methyl-2,4-dioxo-1(2H)-pyrimidinyl)acetyl]-L-phenylalanine (T-phe) and *N*-(2-Aminoethyl)-3,4-dihydro-5-methyl-2,4-dioxo-1(2H)-pyrimidineacetamide (T-NH₂), were designed and synthesized as described in Scheme 1. Following the

procedures reported by Katritzky and coworkers, (thymine-1-yl) acetic acid was prepared by the substitution reaction of T and bromoacetic acid.³⁵ (Thymine-1-yl) acetic acid was subsequently reacted with L-phenylalanine to yield T-phe. Meanwhile, (thymine-1-yl) acetic acid could also react with *N*-Boc-ethylenediamine followed by deprotection to prepare T-NH₂. The molecular structures of T-phe and T-NH₂ were characterized by ¹H NMR and ¹³C NMR spectroscopy. The ¹H NMR spectrum of (thymine-1-yl) acetic acid and the corresponding peak assignments were shown in Supporting Information Figure S1a. After amidation with L-phenylalanine, new signals at 2.89, 3.04, and 7.35 ppm related to T-phe appeared (Supporting Information Fig. S1b). If amidation was carried out with *N*-Boc-ethylenediamine followed by deprotection, it was found in Supporting Information Figure S1c that additional peaks at 2.86 and 3.3 ppm were attributed to T-NH₂. The ¹³C NMR spectra of T-phe and T-NH₂ shown in Supporting Information Figure S2 further confirmed the structure of the target products. Consequently, all

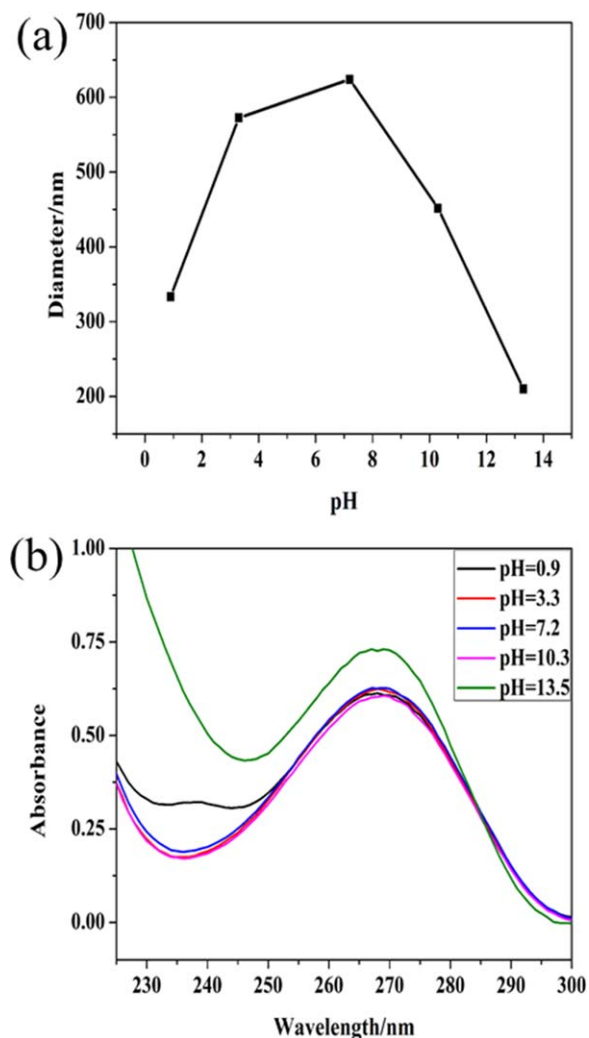


FIGURE 3 (a) Diameters from DLS, (b) UV spectra of mixture of T-phe and T-NH₂ with M at pH 0.9–13.5. [Color figure can be viewed at [wileyonlinelibrary.com](#)]

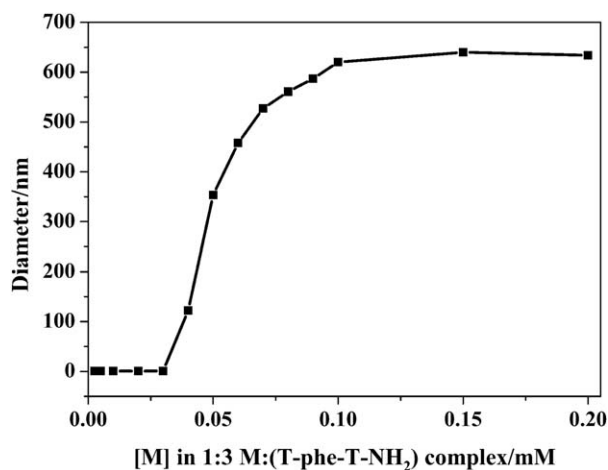


FIGURE 4 Diameters from DLS for T-phe and T-NH₂ with M at various concentrations ranging from 0.0025 mM to 0.2 mM ([M]) in phosphate buffer.

NMR results demonstrated that two derivatives of T bearing terminal amide and carboxyl groups were successfully synthesized.

Self-Assembly Behavior of T-phe, T-NH₂, and M

To optimize the self-assembly condition for three components including M, T-phe, and T-NH₂, DLS and UV/Vis spectrophotometry were used to estimate the assemblies when varying their proportion. First, different M solutions ranging from 0 mM to 0.6 mM were added into the phosphate buffer solution of T-phe (0.15 mM) and T-NH₂ (0.15 mM) based on the molar ratios 0:3, 0.3:3, 0.6:3, 1:3, 3:3, and 6:3. As shown in Figure 1(a), the hydrodynamic diameter of the mixture measured by DLS as a function of the molar ratio of M and T (T-phe and T-NH₂) was plotted. With increasing M concentration, the mixture size dramatically increased from around 50 nm to 680 nm. An equilibrium was found at a molar ratio of 1:3 (1M-3T), which indicated the optimal proportion. The hypochromic effect is reflected by the UV absorption change

in the process of denaturation and renaturation of polynucleotides and nucleic acids, owing to H-bonds and stacking interactions between the bases.^{37,38} Herein, UV absorbance at 270 nm was employed to evaluate the efficiency of base stacking [Fig. 1(b)]. It was found that the peak intensity gradually decreased with increasing M concentration until 1M-3T reached. Therefore, 1M-3T was the appropriate ratio for the mixture, where their self-assembly was pronounced.

Meanwhile, a solution of M (0.1 mM) was added into the phosphate buffer solutions with different molar ratios of T-phe and T-NH₂. The size of the mixture by DLS as a function of the molar ratio of T-phe and T-NH₂ was also plotted and presented in Figure 2(a). When T-phe concentration was gradually increased with a fixed 1M-3T, the dimension was firstly increased and then dropped quickly. When T-phe was equivalent to T-NH₂, a maximum size was reached due to the strongest Coulomb attractive force between amide and carboxyl groups. Figure 2(b) showed the UV spectra of different molar ratios of T-phe and T-NH₂. It was observed that the peak at 270 nm was the lowest when the ratio of T-phe to T-NH₂ was 1.5:1.5 (1.5T-phe-1.5T-NH₂), where the hypochromic effect was the most significant. Consequently, the optimum ratio for the most efficient recognition and base stacking was determined as 1M-1.5T-phe-1.5T-NH₂. It was ascribed that the strongest attraction was resulted from the equivalence of T-phe and T-NH₂, which were interacted with three complementary faces of M.

Self-Assembly at Different pH Values and Concentrations

In the following study, assemblies formed from 1M-1.5T-phe-1.5T-NH₂ were generally applied for other investigations unless otherwise noted. Figure 3(a) revealed the change of assembly size by DLS against pH variation. A maximum size of assemblies was observed at neutral condition (pH 7.2), while both T-phe (pK_a = 3.45, Supporting Information Fig. S3a) and T-NH₂ (pK_a = 9.65, Supporting Information Fig. S3b) were in their charge state. However, the size decreased quickly at either pH < 3.45 (T-phe was uncharged, T-NH₂ was

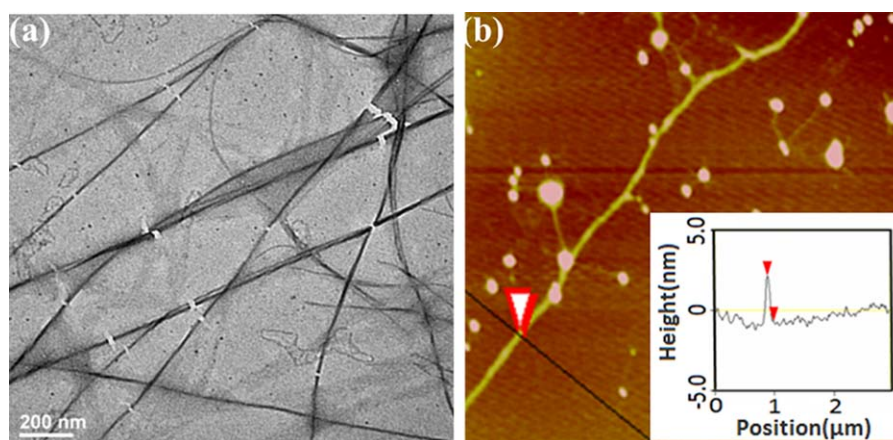
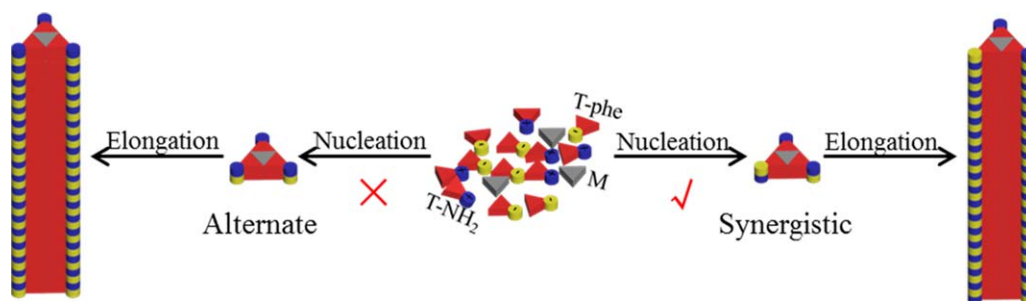


FIGURE 5 Images of T-phe and T-NH₂ with M supramolecular self-assemblies. (a) TEM image and (b) AFM micrograph of self-assembled T-phe and T-NH₂ with M fibers. [M] = 0.1 mM, [T-phe] = [T-NH₂] = 0.15 mM in phosphate buffer. [Color figure can be viewed at wileyonlinelibrary.com]



SCHEME 2 Model of the proposed self-assembly process. [Color figure can be viewed at wileyonlinelibrary.com]

positively charged) or $\text{pH} > 9.65$ (T-phe was negatively charged, T-NH₂ was uncharged) environment owing to the disrupted electrostatic equilibrium. UV spectra of mixture [Fig. 3(b)] further confirmed the change of base stacking under extremely acidic and basic environment. Compared with other curves, it was found that negative band at 236 nm changed sharply at both conditions, indicating the non-efficient self-assembly of M. However, it was also observed a peak arising at 236 nm only for pH at 0.9, which might be caused by free M as shown in Supporting Information Figure S4. Therefore, it could be concluded that the size and base stacking of self-assembly were able to be adjusted by changing solution pH owing to the varying Coulomb attractive forces, which agreed with results reported in literature.¹³

We further investigated the effect of concentration on assemblies by DLS. As described in Figure 4, the hydrodynamic diameter of mixture as a function of the concentration of M was presented. In general, the lower the concentration, the smaller size of the assembly. In particular, a sharp increment of diameter was observed at the concentration of 0.03 mM, which was suggested as the critical concentration for self-assembly of the mixture. Sleiman and coworkers have reported that the process of CA-mediated poly(A) assembly on dilution occurred with a sharp transition as a function of concentration, which indicated a cooperative assembly onset at a critical concentration of the small molecule.²⁵ Therefore, our result presented here hinted that the process of M-driven T derivatives assembly exhibited a similar cooperative nucleation–elongation pathway.

Microscopic Images on Supramolecular Assembly

The morphology of the assemblies was firstly visualized by transmission electron microscopy (TEM) as shown in Figure 5(a), which revealed fiber structures with extremely high aspect ratios in phosphate buffer solution. Furthermore, image from atomic force microscope (AFM) as shown in Figure 5(b) implied the accurate diameter of assemblies. For example, a diameter between 2.6 and 3.2 nm was detected for a single fiber perpendicular to the image plane (i.e., the height). It has also been reported that the diameter of the self-assembly fiber from 2,4,6-triaminopyrimidine modified with succinate group (TAPAS) and cyanuric acid (CA) was between 1.5 and 2.2 nm.³⁹ Moreover, the diameter of the nanotubes from the G \wedge C motif was between 3.1 and 3.7 nm.¹⁸ Thus, it could be speculated that the diameter

presented here was in the range of similar assembled mechanism. A rough calculation was also carried out for an M-3T structure, which included 1.2 nm as reported non-substitution³⁹ plus approximately 1.5 nm substitution. So a theoretical diameter of 2.7 nm for the assemblies was estimated, in accordance with the AFM results.

Proposed Mechanism for Supramolecular Assembly

Herein, M-driven nucleobase derivatives assembly *via* non-covalent interactions led to the fibrous structure, suggesting that the process was close to a supramolecular polymerization.^{40,41} It may thus occur *via* two distinct mechanisms: isodesmic (step-growth) or cooperative polymerization (nucleation–growth).⁴² The self-assembly at different concentrations (Fig. 4) showed that the self-assembly only occurred above a critical concentration, which was more inclined to cooperative nucleation–growth polymerization.^{25,43} Considering the fiber's diameter of the supramolecular structure, we proposed that in the nucleation process tetrameric structures formed by multiple hydrogen bonds between M and T, which was consistent with the literature.⁴⁴ Subsequently, the tetrameric structures were extended by π -stacking and electrostatic interaction during the elongation process.

However, the tetrameric structures may differ in the nucleation process. As illustrated in Scheme 2, there were two

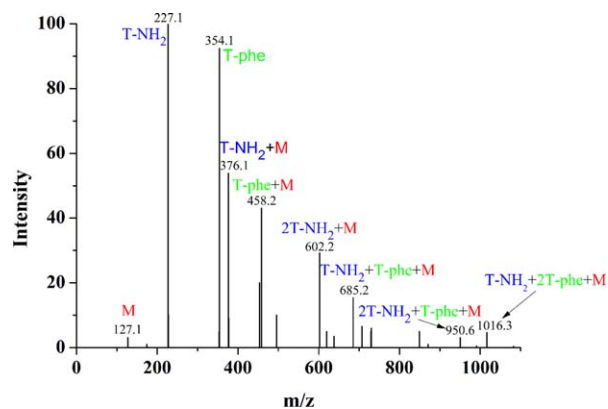


FIGURE 6 ESI-MS of a 0.1 mM solution of T-phe and T-NH₂ with M. The peaks at 127.1, 227.1, 354.1, 376.1, 458.2, 602.2, 685.2, 950.6, and 1016.3 corresponded to the non-covalent intermediate species of the self-assembled structures (1-mer to 4-mer). [Color figure can be viewed at wileyonlinelibrary.com]

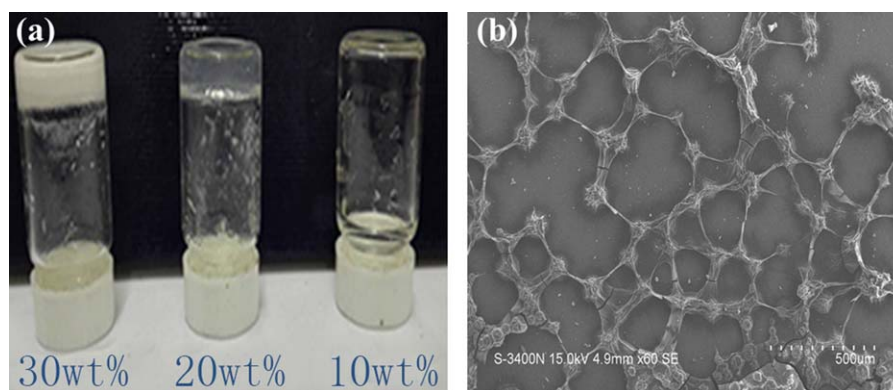


FIGURE 7 (a) Inverted bottle test demonstrating gelation as a function of concentration. Each solution kept the ratio of [M]:[T] (1:3) unchanged while [T-phe] was equal to [T-NH₂], all buffered at pH 7.2, (b) SEM image of self-assembled T-phe + T-NH₂ with M gel at 20 wt %. [Color figure can be viewed at wileyonlinelibrary.com]

possible combinations including 1M-3T-phe/1M-3T-NH₂ (alternate self-assembly) and 1M-2T-phe-1T-NH₂/1M-T-phe-2T-NH₂ (synergistic self-assembly) in view of the repulsive or attractive Coulomb interactions.¹³ To confirm the nucleation process, electrospray ionization mass spectrometry (ESI-MS) was conducted to investigate the composition of the non-covalent intermediate species (1-mer to 4-mer) of the parent tetrameric structure. As shown in Figure 6, two-weak signals at $m/z = 950.6$ [1M-T-phe-2T-NH₂ + H₂O + Na]⁺ and $m/z = 1016.3$ [1M-2T-phe-1T-NH₂ + H]⁺ were found. In contrast, the signals of 1M-3T-phe and 1M-3T-NH₂ were not shown, possibly attributing to the concentrated charge of 3T-phe-M or 3T-NH₂-M. Therefore, it was suggested that the process preferred to occur through a synergistic rather than an alternate self-assembly.

Gelation of the Supramolecular Assembly

It has been known that DAP-Cyco4 assemblies formed linear fibers in dilute solutions and a metastable hydrogel in concentrated solutions.²⁶ Therefore, we hypothesized that fibrillar structure presented here could also generate hydrogels at high concentrations. To verify the assumption, the concentrations of M, T-phe, and T-NH₂ were further increased at their optimized ratio. As determined by the test tube inversion method, assemblies displayed critical gel concentration (CGC) at 20 wt %. Further increasing the concentrations to 30 wt % led to an opaque hydrogel [Fig. 7(a)], which was attributed to the poor solubility of M. However, 30 wt % solution of T-phe and T-NH₂ in water without M was not able to form gel (Supporting Information Fig. S5). Furthermore, SEM image of the transparent hydrogel was presented in Figure 7(b), which revealed a highly branched network of interlinked fibers owing to the entanglement. This observation was consistent with the formation of non-covalent cross-linked supramolecular assemblies.²⁶ Consequently, the self-assembly system presented here demonstrated that the nucleobase-based complex could be used as a building block to generate hydrogels, which would be favorable for bio-inspired material design and applications.

CONCLUSIONS

In summary, T-phe and T-NH₂, bearing the terminal amide and carboxyl group respectively, have been successfully synthesized. The optimal condition for self-assembly of T-phe and T-NH₂ driven by M was determined at 1M-1.5T-phe-1.5T-NH₂ under neutral environment. These molecules self-assembled into fibrous supramolecular structure with a few nanometers in diameter. It was preliminarily demonstrated that the self-assembly process was similar to cooperative nucleation-growth polymerization and the nucleation process was mainly promoted by synergistic self-assembly. Moreover, hydrogels could be spontaneously generated with increased concentrations of building molecules of T and M at their optimized ratio. This efficient self-assembly system based on biomimetic compounds would have great potential in supramolecular polymers and bio-inspired materials.

ACKNOWLEDGMENTS

This work was supported by the National Natural Science Foundation of China (21674037) and the Shanghai Scientific and Technological Innovation Project (14520720600).

REFERENCES AND NOTES

- 1 C. Fouquey, J. M. Lehn, A. M. Levelut, *Adv. Mater.* **1990**, *2*, 254.
- 2 Z. Zhang, L. Shao, Y. Zhou, J. Yang, *J. Polym. Sci. Part A: Polym. Chem.* **2017**, *55*, 3529.
- 3 A. J. P. Teunissen, J. A. Berrocal, C. Corbet, E. W. Meijer, *J. Polym. Sci. Part A: Polym. Chem.* **2017**, *55*, 2971.
- 4 W. Seo, K. L. Carpenter, J. A. Gaugler, W. Shao, K. A. Werling, P. M. Fournier, D. S. Lambrecht, A. Star, *J. Polym. Sci. Part A: Polym. Chem.* **2017**, *55*, 1095.
- 5 B. J. B. Folmer, R. P. Sijbesma, R. M. Versteegen, J. A. J. van der Rijt, E. W. Meijer, *Adv. Mater.* **2000**, *12*, 874.
- 6 J. M. Zayed, N. Nouvel, U. Rauwald, O. A. Scherman, *Chem. Soc. Rev.* **2010**, *39*, 2806.
- 7 E. Krieg, M. M. Bastings, P. Besenius, B. Rybtchinski, *Chem. Rev.* **2016**, *116*, 2414.

- 8 P. Y. W. Dankers, T. M. Hermans, T. W. Baughman, Y. Kamikawa, R. E. Kieltyka, M. M. C. Bastings, H. M. Janssen, N. A. J. M. Sommerdijk, A. Larsen, M. J. A. van Luyn, A. W. Bosman, E. R. Popa, G. Fytas, E. W. Meijer, *Adv. Mater.* **2012**, *24*, 2703.
- 9 E. Obert, M. Bellot, L. Bouteiller, F. Andrioletti, C. Lehen-Ferrenbach, F. Boué, *J. Am. Chem. Soc.* **2007**, *129*, 15601.
- 10 T. H. Rehm, C. Schmuck, *Chem. Soc. Rev.* **2010**, *39*, 3597.
- 11 N. Jiang, J. Shang, X. Di, M. K. Endoh, T. Koga, *Macromolecules* **2014**, *47*, 2682.
- 12 Q. He, S. Narayanan, D. T. Wu, M. D. Foster, *ACS Macro Lett.* **2016**, *5*, 999.
- 13 H. Frisch, J. P. Unsleber, D. Ludeker, M. Peterlechner, G. Brunklau, M. Waller, P. Besenius, *Angew. Chem. Int. Ed. Engl.* **2013**, *52*, 10097.
- 14 R. C. Howe, A. P. Smalley, A. P. Guttenplan, M. W. Doggett, M. D. Eddleston, J. C. Tan, G. O. Lloyd, *Chem. Commun.* **2013**, *49*, 4268.
- 15 J. L. Sessler, C. M. Lawrence, J. Jayawickramarajah, *Chem. Soc. Rev.* **2007**, *36*, 314.
- 16 H. Fenniri, P. Mathivanan, K. L. Vidale, D. M. Sherman, K. Hallenga, K. V. Wood, J. G. Stowell, *J. Am. Chem. Soc.* **2001**, *123*, 3854.
- 17 J. G. Moralez, J. Ruez, T. Yamazaki, R. K. Motkuri, A. Kovalenko, H. Fenniri, *J. Am. Chem. Soc.* **2005**, *127*, 8307.
- 18 G. Borzsonyi, R. L. Beingsner, T. Yamazaki, J.-Y. Cho, A. J. Myles, M. Malac, R. Egerton, M. Kawasaki, K. Ishizuka, A. Kovalenko, H. Fenniri, *J. Am. Chem. Soc.* **2010**, *132*, 15136.
- 19 D. Wang, Y. Su, C. Jin, B. Zhu, Y. Pang, L. Zhu, J. Liu, C. Tu, D. Yan, X. Zhu, *Biomacromolecules* **2011**, *12*, 1370.
- 20 P. O. P. Ts'ou, I. S. Melvin, A. C. Olson, *J. Am. Chem. Soc.* **1962**, *85*, 1289.
- 21 J. T. Davis, *Angew. Chem. Int. Ed. Engl.* **2004**, *43*, 668.
- 22 Y. Yu, D. Nakamura, K. Deboyace, A. W. Neisius, L. B. McGown, *J. Phys. Chem. B* **2008**, *112*, 1130.
- 23 D. Chandler, *Nature* **2005**, *437*, 640.
- 24 B. J. Cafferty, N. V. Hud, *Isr. J. Chem.* **2015**, *55*, 891.
- 25 N. Avakyan, A. A. Greschner, F. Aldaye, C. J. Serpell, V. Toader, A. Petitjean, H. F. Sleiman, *Nat. Chem.* **2016**, *8*, 368.
- 26 C. Li, B. J. Cafferty, S. C. Karunakaran, G. B. Schuster, N. V. Hud, *Phys. Chem. Chem. Phys.* **2016**, *18*, 20091.
- 27 B. Roy, P. Bairi, A. K. Nandi, *RSC Adv.* **2014**, *4*, 1708.
- 28 J. Xu, G. Wu, Z. Wang, X. Zhang, *Chem. Sci.* **2012**, *3*, 3227.
- 29 S. Yagai, M. Usui, T. Seki, H. Murayama, Y. Kikkawa, S. Uemura, T. Karatsu, A. Kitamura, A. Asano, S. Shu, *J. Am. Chem. Soc.* **2012**, *134*, 7983.
- 30 W. J. Qi, D. Wu, J. Ling, C. Z. Huang, *Chem. Commun.* **2010**, *46*, 4893.
- 31 Y. Tao, Y. Yang, D. Shi, M. Chen, C. Yang, X. Liu, *Polymer* **2012**, *53*, 1551.
- 32 Y. Zeng, Y. Pratumyot, X. Piao, D. Bong, *J. Am. Chem. Soc.* **2012**, *134*, 832.
- 33 X. Piao, X. Xia, D. Bong, *Biochemistry* **2013**, *52*, 6313.
- 34 J. Mao, C. DeSantis, D. Bong, *J. Am. Chem. Soc.* **2017**, *139*, 9815.
- 35 A. R. Katritzky, T. Narindoshvili, *Org. Biomol. Chem.* **2008**, *6*, 3171.
- 36 X. Li, Y. Kuang, J. Shi, Y. Gao, H. C. Lin, B. Xu, *J. Am. Chem. Soc.* **2011**, *133*, 17513.
- 37 M. Gentner, M. G. Allan, F. Zaehring, T. Schirmer, S. Grzesiek, *J. Am. Chem. Soc.* **2012**, *134*, 1019.
- 38 V. I. Danilov, *FEBS Lett.* **1974**, *47*, 155.
- 39 B. J. Cafferty, I. Gallego, M. C. Chen, K. I. Farley, R. Eritja, N. V. Hud, *J. Am. Chem. Soc.* **2013**, *135*, 2447.
- 40 P. Besenius, *J. Polym. Sci. Part A: Polym. Chem.* **2017**, *55*, 34.
- 41 L. Brunsveld, B. Folmer, E. Meijer, R. Sijbesma, *Chem. Rev.* **2001**, *101*, 4071.
- 42 S. Ogi, T. Fukui, M. L. Jue, M. Takeuchi, K. Sugiyasu, *Angew. Chem. Int. Ed. Engl.* **2014**, *53*, 14363.
- 43 T. F. A. D. Greef, M. M. J. Smulders, M. Wolffs, A. P. H. J. Schenning, R. P. Sijbesma, E. W. Meijer, *Chem. Rev.* **2009**, *109*, 5687.
- 44 R. F. Lange, F. H. Beijer, R. P. Sijbesma, R. W. Hooft, H. Kooijman, A. L. Spek, J. Kroon, E. Meijer, *Angew. Chem. Int. Ed. Engl.* **1997**, *36*, 969.